

Contribution from the Department of Chemistry,
University of Virginia, Charlottesville, Virginia 22901

Crystal and Molecular Structures of Six Five-Coordinated Binuclear Copper(II) Complexes of Gradually Varying Geometry. Relation between Ligand Electronegativity, Steric Constraints, and Structures

EKK SINK

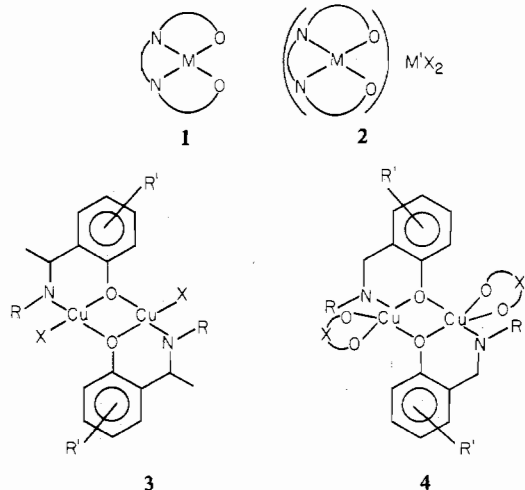
Received December 2, 1975

AIC50861A

A series of binuclear copper(II) complexes have been synthesized from bidentate salicylaldimines with nitrogen (R) and ring (R') substituents and another bidentate ligand (X). The complexes were studied by single-crystal x-ray diffraction using counter methods and their structures were determined. Crystal data are as follows: (a) bis[nitrato(*N*-*n*-propyl-2-hydroxybenzylideniminato- μ -O)copper(II)], Cu₂O₈N₄C₂₈H₂₈, X = NO₃, R = *n*-propyl, R' = 5,6-benzo, space group P $\bar{1}$, Z = 1, a = 10.420 (3) Å, b = 8.489 (8) Å, c = 11.687 (2) Å, α = 107.38 (6)°, β = 90.96 (2)°, γ = 131.19 (8)°, V = 709 Å³, R = 5.6%, 2142 reflections; (b) bis[4,4,4-trifluoro-1-(2-thienyl)-1,3-butanedionato(*N*-(2-methylethyl)-2-hydroxybenzylideniminato- μ -O)copper(II)], Cu₂S₂F₆O₆N₂C₃₆H₃₂, X = thenoyltrifluoroacetylacetone (thac), R = isopropyl, R' = H, space group P $\bar{1}$, Z = 1, a = 7.978 (2) Å, b = 11.031 (1) Å, c = 12.399 (3) Å, α = 117.89 (2)°, β = 100.46 (2)°, γ = 92.65 (2)°, V = 938 Å³, R = 3.6%, 2676 reflections; (c) bis[1,1,1,5,5-hexafluoro-2,4-pentanedionato(*N*-phenyl-2-hydroxybenzylideniminato- μ -O)copper(II)], Cu₂F₁₂O₆N₂C₃₂H₂₂, X = hexafluoroacetylacetone (hfa), R = phenyl, R' = H, space group P $\bar{1}$, Z = 1, a = 9.066 (1) Å, b = 10.583 (3) Å, c = 10.710 (6) Å, α = 99.64 (3)°, β = 114.33 (3)°, γ = 94.58 (2)°, V = 910 Å³, R = 5.1%, 2642 reflections; (d) bis[1,1,1,5,5-hexafluoro-2,4-pentanedionato(*N*-ethyl-5-chloro-2-hydroxybenzylideniminato- μ -O)copper(II)], Cu₂Cl₂F₁₂O₆N₂C₂₈H₂₀, X = hfa, R = ethyl, R' = 5-Cl, space group P $\bar{1}$, Z = 1, a = 9.044 (3) Å, b = 9.300 (3) Å, c = 12.432 (4) Å, α = 95.46°, β = 117.51°, γ = 108.14 (2)°, V = 845 Å³, R = 3.5%, 2392 reflections; (e) bis[1,1,1,5,5-hexafluoro-2,4-dionato(*N*-(2-methylethyl)-2-hydroxybenzylideniminato- μ -O)copper(II)], Cu₂F₁₂O₆N₂C₃₀H₂₆, X = hfa, R = isopropyl, R' = H, space group P₂₁/c, Z = 2, a = 12.142 (3) Å, b = 16.104 (6) Å, c = 8.835 (1) Å, β = 94.88 (1)°, V = 1721 Å³, R = 4.9%, 2389 reflections; (f) bis[1,1,1,5,5-hexafluoro-2,4-pentanedionato(*N*-(2,2-dimethylethyl)-2-hydroxybenzylideniminato- μ -O)copper(II)], Cu₂F₁₂O₆N₂C₃₂H₂₈, X = hfa, R = *tert*-butyl, R' = H, space group P₂₁/c, Z = 2, a = 8.918 (3) Å, b = 12.776 (3) Å, c = 16.674 (4) Å, β = 103.57 (2)°, V = 1847 Å³, R = 6.4%, 1723 reflections. The metal atoms are five-coordinated, with four stronger and one weaker bond in each case, but the binucleation ranges from A pairs of (distorted) square pyramids joined at the edges of their coplanar bases to B pairs of square pyramids joined at the apices. Between the two extremes (A and B), the distortion toward trigonal-bipyramidal geometry is strongest. The strengths of the bridging bonds and the coplanarity of the pyramid bases (and hence the strength of antiferromagnetic exchange interactions) increase with increasing electronegativity of ligand X. This trend is observed independently of steric constraints, but an additional trend from A to B is observed with decreasing bulkiness of X for a limited sample and with other factors kept constant.

Introduction

It is well-known that tetradeятate Schiff base (TSB) complexes (**1**) can act as ligands to form bi- and trinuclear



complexes¹ (**2**, n = 1, 2; X = Cl, Br, NO₃, ClO₄) and that 2,2'-bipyridine (bpy) analogues such as 2,2'-biquinoline act as approximate steric models for the TSB in forming such complexes.² Complex ligands **1** have been adducted to metal halides, nitrates, and perchlorates. Copper(II) β -diketonates can also form adducts with extra ligands³⁻¹¹ including bpy⁹ and a variety of other bidentate ligands.^{10,11} This works especially well with hfa (hexafluoroacetylacetone).⁷ Consequently, type **2** complexes with X = hfa, n = 1 (and M = M' = Cu, for example) are expected and observed.¹² A related complex, with TSB = N,N'-ethylenebis(salicylaldimine), X

= hfa, n = 1, M = Cu, M' = Co, has already been characterized.¹³ For every complex of type **2**, n = 1, M = M' = Cu, a corresponding trans-bridged complex such as **3** (X monodentate) and **4** (X bidentate) is expected and observed¹⁴⁻¹⁶ for bidentate Schiff base complexes (BSB). Thus type **4** complexes, with X a β -diketone¹⁸ or nitrate^{16,17,19} are known, and a comparison of the structural features of several such complexes is presented here.

Experimental Section

The synthesis of the β -diketone and BSB complexes is described elsewhere.²⁰ Crystals of the binuclear complexes were prepared by adding the solid copper β -diketonate or copper nitrate hexahydrate to a hot stirred saturated solution of the appropriate CuBSB complex in triethoxymethane and allowing the resulting solution to stand for a few days. The complexes studied here are as follows: **4a**, X = NO₃, R = *n*-propyl, R' = 5,6-benzo; **4b**, X = thenoyltrifluoroacetylacetone, thac, R = isopropyl, R' = H; **4c**, X = hfa, R = phenyl, R' = H; **4d**, X = hfa, R = ethyl, R' = 5-Cl; **4e**, X = hfa, R = isopropyl, R' = H; **4f**, X = hfa, R = *tert*-butyl, R' = H.

Crystal Data for 4a, Bis[nitrato(*N*-*n*-propyl-2-hydroxybenzylideniminato- μ -O)copper(II)], [Cu(PrNaph)NO₃]₂: Cu₂O₈N₄C₂₈H₂₈, mol wt 676, space group P $\bar{1}$, Z = 1, a = 10.420 (3) Å, b = 8.489 (8) Å, c = 11.687 (2) Å, α = 107.38 (6)°, β = 90.96 (2)°, γ = 131.19 (8)°, V = 709 Å³, μ (Mo K α) = 16.3 cm⁻¹, ρ_{calcd} = 1.60 g cm⁻³, ρ_{obsd} = 1.58 g cm⁻³; crystal was approximately a spherical fragment with no discernible faces, diameter 0.12 mm; spherical absorption corrections were used, maximum transmission = minimum transmission = 0.87.

Crystal Data for 4b, Bis[4,4,4-trifluoro-1-(2-thienyl)-1,3-butanedionato(*N*-(2-methylethyl)-2-hydroxybenzylideniminato- μ -O)copper(II)], [Cu(i-PrSal)thac]₂: Cu₂S₂F₆O₆N₂C₃₆H₃₂, mol wt 894, space group P $\bar{1}$, Z = 1, a = 7.978 (2) Å, b = 11.031 (1) Å, c = 12.399 (3) Å, α = 117.89 (2)°, β = 100.46 (2)°, γ = 92.65 (2)°, V = 938 Å³, μ (Mo K α) = 13.7 cm⁻¹, ρ_{calcd} = 1.59 g cm⁻³, ρ_{obsd} = 1.56 g cm⁻³; crystal dimensions (distance in mm from centroid) (100) 0.25, (100) 0.25, (010) 0.155, (010) 0.155, (001) 0.10, (001) 0.10; max, min transmission = 0.85, 0.72.

Crystal Data for 4c, Bis[1,1,1,5,5-hexafluoro-2,4-pentanedionato(*N*-phenyl-2-hydroxybenzylideminato- μ -*O*)copper(II)], [Cu(PhSal)hfa]₂: Cu₂F₁₂O₆N₂C₃₆H₂₂, mol wt 934, space group P $\bar{1}$, Z = 1, a = 9.066 (1) Å, b = 10.583 (3) Å, c = 10.710 (6) Å, α = 99.64 (3) $^\circ$, β = 114.33 (3) $^\circ$, γ = 94.58 (2) $^\circ$, V = 910 Å³, μ (Mo K α) = 13.5 cm⁻¹, ρ_{calcd} = 1.72 g cm⁻³, ρ_{obsd} = 1.68 g cm⁻³; crystal dimensions (mm from centroid) (001) 0.10; (001) 0.10; (010) 0.125, (010) 0.125, (201) 0.34, (201) 0.34; max, min transmission = 0.84, 0.78.

Crystal Data for 4d, Bis[1,1,1,5,5-hexafluoro-2,4-pentanedionato(*N*-ethyl-5-chloro-2-hydroxybenzylideminato- μ -*O*)copper(II)], [Cu(Et-5-ClSal)hfa]₂: Cu₂Cl₂F₁₂O₆N₂C₂₈H₂₀, mol wt 906, space group P $\bar{1}$, Z = 1, a = 9.044 (3) Å, b = 9.300 (3) Å, c = 12.432 (4) Å, α = 95.46 (2) $^\circ$, β = 117.51 (2) $^\circ$, γ = 108.14 (2) $^\circ$, V = 845 Å³, μ (Mo K α) = 16.3 cm⁻¹, ρ_{calcd} = 1.84 g cm⁻³, ρ_{obsd} = 1.85 g cm⁻³; crystal dimensions (mm from centroid) (001) 0.135, (001) 0.135, (101) 0.13, (101) 0.13, (010) 0.35, (010) 0.35, (110) 0.35, (110) 0.35; max, min transmission = 0.78, 0.72.

Crystal Data for 4e, Bis[1,1,1,5,5-hexafluoro-2,4-pentanedionato(*N*-(2-methylethyl)-2-hydroxybenzylideminato- μ -*O*)copper(II)], [Cu(i-PrSal)hfa]₂: Cu₂F₁₂O₆N₂C₃₀H₂₆, mol wt 866, space group P $\bar{1}$ /c, Z = 2, a = 12.142 (3) Å, b = 16.104 (6) Å, c = 8.835 (1) Å, β = 94.88 (1) $^\circ$, V = 1721 Å³, μ (Mo K α) = 14.1 cm⁻¹, ρ_{calcd} = 1.68 g cm⁻³, ρ_{obsd} = 1.71 g cm⁻³; crystal dimensions (mm from centroid) (100) 0.08, (100) 0.08, (010) 0.225, (010) 0.225, (011) 0.20, (011) 0.20, (011) 0.19, (011) 0.19; max, min transmission = 0.85, 0.69.

Crystal Data for 4f, Bis[1,1,1,5,5-hexafluoro-2,4-pentanedionato(*N*-(2,2-dimethylethyl)-2-hydroxybenzylideminato- μ -*O*)copper(II)], [Cu(t-BuSal)hfa]₂: Cu₂F₁₂O₆N₂C₃₂H₂₈, mol wt 894, space group P $\bar{1}$ /c, Z = 2, a = 8.918 (3) Å, b = 12.776 (3) Å, c = 16.674 (4) Å, β = 103.57 (2) $^\circ$, V = 1847 Å³, μ (Mo K α) = 13.1 cm⁻¹, ρ_{calcd} = 1.61 g cm⁻³, ρ_{obsd} = 1.63 g cm⁻³; crystal dimensions (mm from centroid) (100) 0.04, (100) 0.05, (010) 0.06, (010) 0.06, (001) 0.06, (001) 0.06; max, min transmission = 0.87, 0.84.

To forestall a slight sensitivity to humid air, the crystals were sealed inside glass capillaries. For each crystal, the Enraf-Nonius program SEARCH was used to obtain 15 accurately centered reflections which were then used in the program INDEX to obtain an orientation matrix for data collection and also approximate cell dimensions. The cell parameters matched those obtained from precession photographs. Refined cell dimensions and their estimated standard deviations were obtained from least-squares refinement of 28 accurately centered reflections. The mosaicity of each crystal was examined by the ω scan technique and judged to be satisfactory.

Collection and Reduction of Diffraction Data. Diffraction data were collected at 292 K on an Enraf-Nonius four-circle CAD-4 diffractometer controlled by a PDP8/M computer using Mo K α radiation from a highly oriented graphite crystal monochromator. The $\theta-2\theta$ scan technique was used to record the intensities for which $1^\circ < 2\theta < 46^\circ$ for **4a** and **4f** and $1^\circ < 2\theta < 48^\circ$ for **4b**, **4c**, **4d**, and **4e**. Scan widths (SW) were calculated from the formula $SW = A + B \tan \theta$ where A is estimated from the mosaicity of the crystal and B allows for the increase in width of peak due to K α_1 and K α_2 splitting. The values of A and B were 0.6° and 0.2°, respectively, for **4d** and **4e**, 0.7° and 0.2° for **4b**, and 0.9° and 0.3° for **4a**, **4c**, and **4f**. This calculated scan angle is extended at each side by 25% for background determination (BG1 and BG2). The net count (NC) is then calculated as $NC = TOT - 2(BG1 + BG2)$ where TOT is the estimated peak intensity. Reflection data were considered insignificant if intensities registered less than 10 counts above background on a rapid prescan, such reflections being rejected automatically by the computer.

The intensities of four standard reflections, monitored for each crystal at 100 reflection intervals, showed no greater fluctuations during the data collection than those expected from Poisson statistics, except that **4a** appeared to lose intensity gradually, totaling 3% over the period of data collection. The data were scaled from the period standard reflection scans using the program CHORTA (K. O. Hodgson, Stanford University), which allows for anisotropic intensity variation. The raw intensity data were corrected for Lorentz-polarization effects and for absorption. After averaging the intensities of equivalent reflections, the data were reduced to 2256 independent intensities for **4a**, 2774 for **4b**, 2742 for **4c**, 2537 for **4d**, 2537 for **4e**, and 2106 for **4f**, of which 2142, 2676, 2642, 2392, 2389, and 1724, respectively, had $F_o^2 > 3\sigma(F_o^2)$, where $\sigma(F_o^2)$ was estimated from counting statistics.²¹ These data were used in the final refinement of the structural parameters.

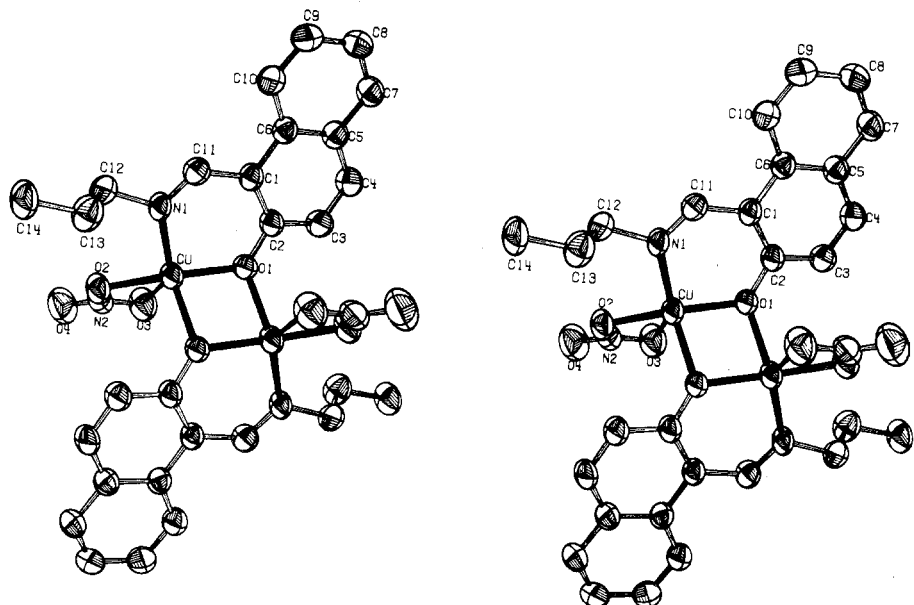
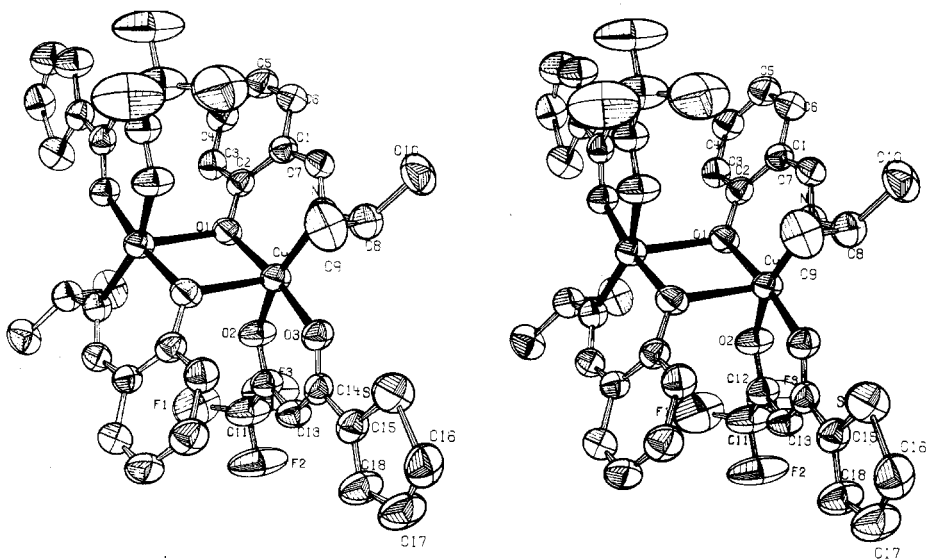
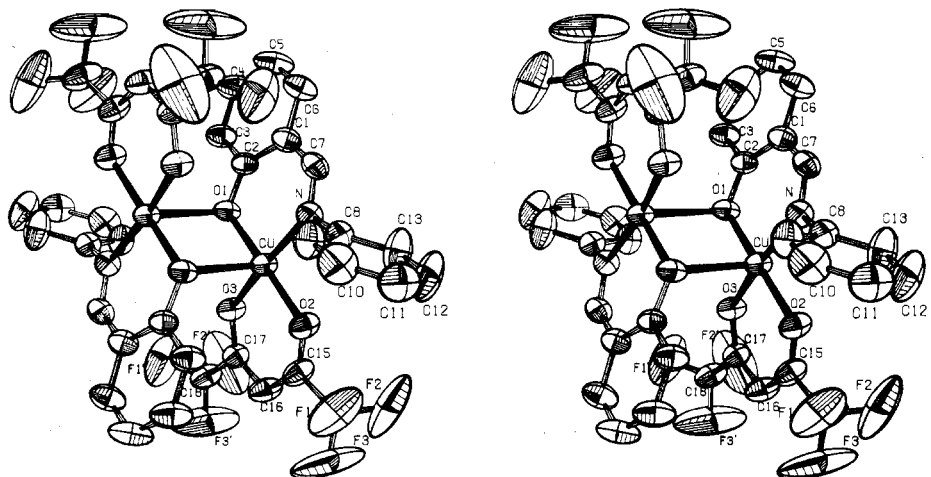
Solution and Refinement of the Structures. In each case the coppers, the bridging oxygens, and some of the other heavier atoms were located from a three-dimensional Patterson synthesis: O(2), O(3) for **4a**; S for **4b**; O(2) for **4c**, **4d**; O(2), O(3) for **4e**, **4f**.

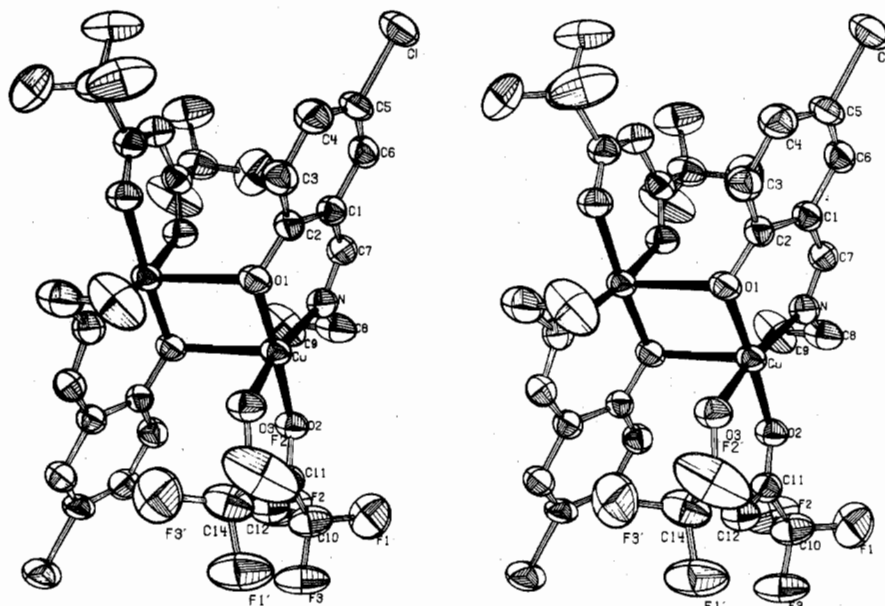
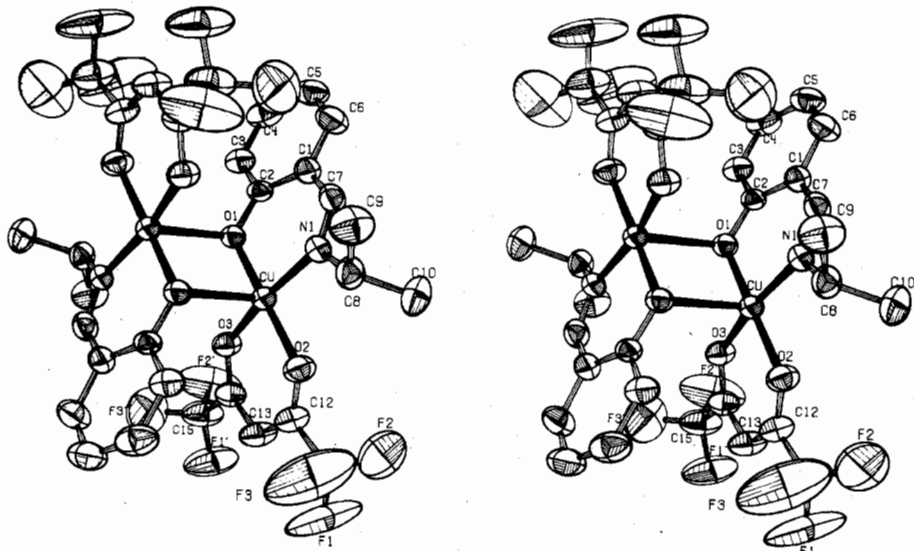
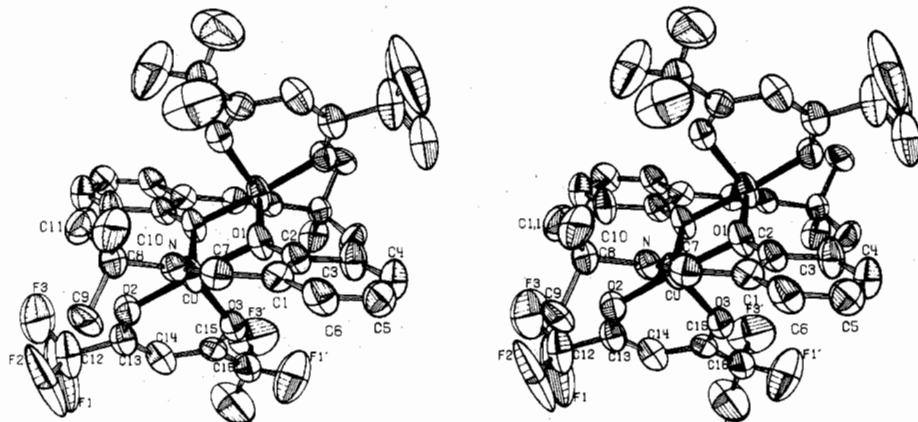
Full-matrix least-squares refinement was based on F, and the function was minimized as $\sum w(F_o - |F_c|)^2$. The weights w were taken as $(2F_o/\sigma(F_o^2))^2$, where |F_o| and |F_c| are the observed and calculated structure factor amplitudes. The atomic scattering factors for nonhydrogen atoms were taken from Cromer and Waber²² and those for hydrogen from Stewart et al.²³ The effects of anomalous dispersion for nonhydrogen atoms were included in F_c using Cromer and Ibers' values²⁴ for $\Delta f'$ and $\Delta f''$. Agreement factors are defined as $R = \sum |F_o| - |F_c| / \sum |F_o|$ and $R_w = (\sum w(|F_o| - |F_c|)^2 / \sum w|F_o|^2)^{1/2}$. To minimize computer time, the initial calculations were carried out on the first 1000 reflections collected. The computing system and programs used were as described elsewhere.²⁵ The intensity data were phased sufficiently well by the "heavy"-atom positions determined in the Patterson map to permit location of the remaining nonhydrogen atoms by difference Fourier syntheses. After full-matrix least-squares refinements, the models converged with $R = 11.0\%$, 8.1%, 9.8%, 6.9%, 9.5%, and 10.8% for **4a**–**4f**, respectively. The remaining diffraction data were added to the calculation, and anisotropic temperature factors were introduced for all nonhydrogen atoms. In each case, Fourier difference maps located hydrogen atoms at the expected positions, in addition to some positional disorder in the CF₃ positions in **4b**, **4c**, **4e**, and **4f**. None of the peaks occurring in the CF₃ groups were higher than 0.7 e Å⁻³ and corresponded to rotations about the C–CF₃ bond, analogous to disorder noted previously in hfa complexes.^{8,11,26} Since the major purpose of this work was the determination of the molecular structures, the disorder was not pursued further (the same procedure having been followed by other workers^{8,11} for the same reasons¹¹). Except for **4a**, the nonmethyl hydrogen atoms and the methyl hydrogen atoms for **4f** were inserted at the calculated positions, with isotropic temperature factors of 5.0 Å², assuming C–H = 0.95 Å. After convergence of these models, the hydrogen atoms were inserted at their new calculated positions. For **4a**, all of the hydrogen atom positions (including methyls) were inserted from the Fourier map and, after two cycles of full-matrix least-squares refinement, held fixed for subsequent cycles. The models converged with $R = 5.6\%$, $R_w = 6.6\%$ for **4a**, $R = 3.6\%$, $R_w = 4.6\%$ for **4b**, $R = 5.1\%$, $R_w = 6.8\%$ for **4c**, $R = 3.4\%$, $R_w = 4.5\%$ for **4d**, $R = 4.9\%$, $R_w = 6.1\%$ for **4e**, and $R = 6.4\%$, $R_w = 7.3\%$ for **4f**. The error in an observation of unit weight is 6.5, 3.4, 4.8, 4.5, 5.9, 3.2 for **4a**–**4f**, respectively. A structure factor calculation with all observed and unobserved reflections included (no refinement) gave $R = 6.2\%$, 4.5%, 5.4%, 3.7%, 5.2%, 7.8% for **4a**–**4f**; on this basis it was decided that careful measurement of reflections rejected automatically during data collection would not significantly improve the results. Tables of the observed structure factors are available.²⁷

Results and Discussion

Final positional and thermal parameters for complexes **4a**–**4f** are given in Tables I–VI. Tables VII and VIII contain the bond lengths and angles. The digits in parentheses in the tables are the estimated standard deviations in the least significant figure quoted and were derived from the inverse matrix in the course of least-squares refinement calculations. Figures 1–6 are stereoscopic pair views of the dimeric molecules, while Figures 7–12 show the molecular packing in the unit cells. Table IX gives the closest intermolecular distances in the cells.

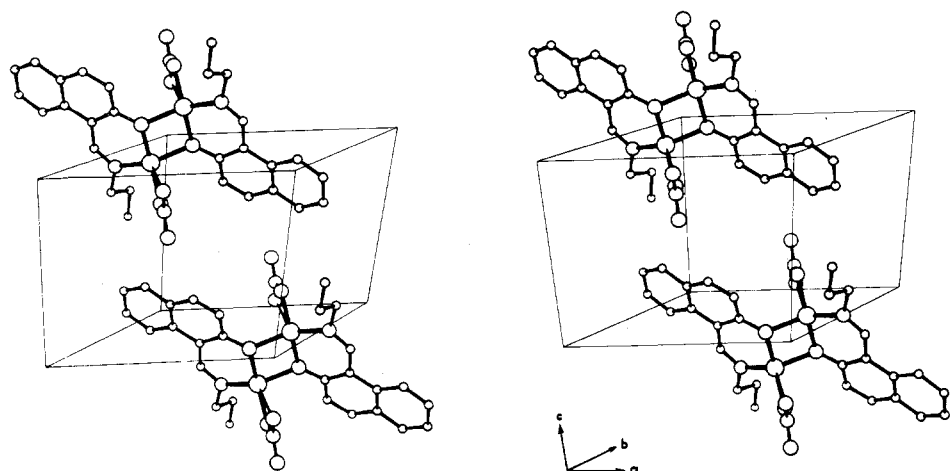
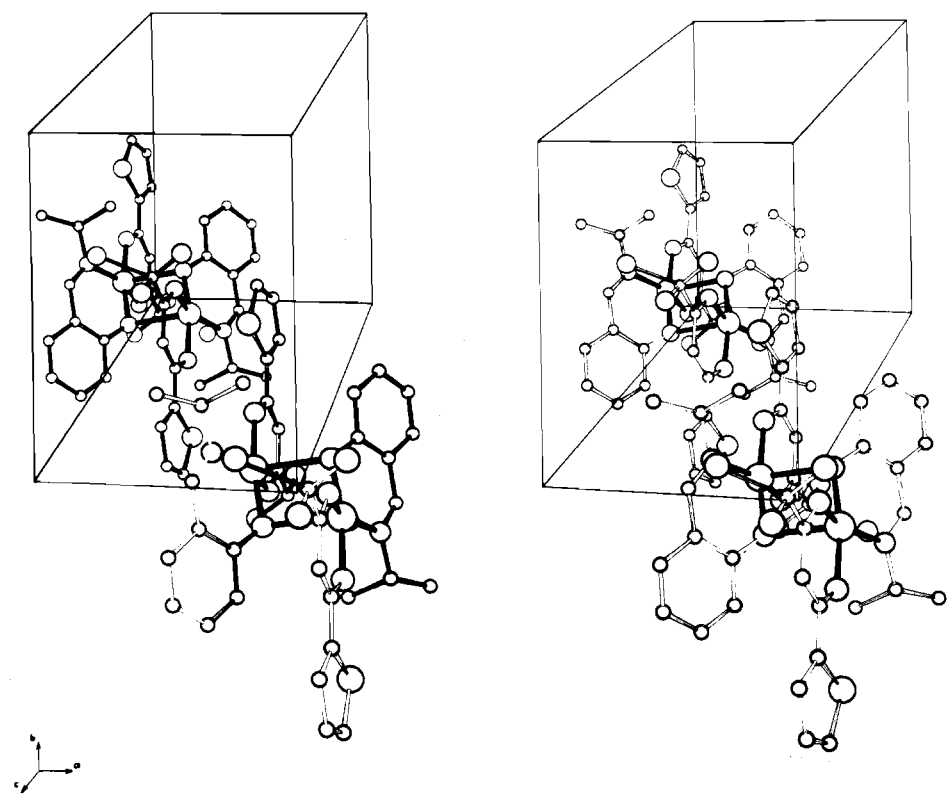
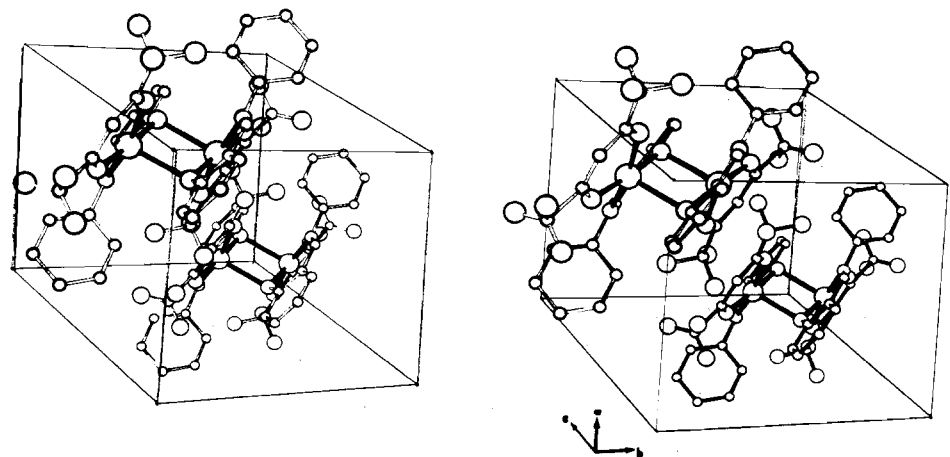
Complex **4a**, [Cu(PrNaph)NO₃]₂, consists of discrete dimeric molecules, the closest intermolecular contacts (3.44–3.48 Å) being between nitrate oxygen atoms and the naphthyl carbons of adjacent molecules. The nitrate group is chelated to the metal with a short (1.91 Å) Cu–O distance in the plane of a rather distorted square pyramid and a very long (2.46 Å) Cu–O bond at the off-center apex of the pyramid. The base [O(1), O(1'), O(2), N(1)] of the pyramid is distorted somewhat (Table X) from planar toward tetrahedral, and the copper atom lies 0.11 Å above this distorted plane. Thus the geometry about the metal atom can also be viewed as a very distorted trigonal bipyramidal or (by ignoring the weak Cu–O bond) as a tetrahedrally distorted square plane. The dimeric molecule consists of the two distorted square

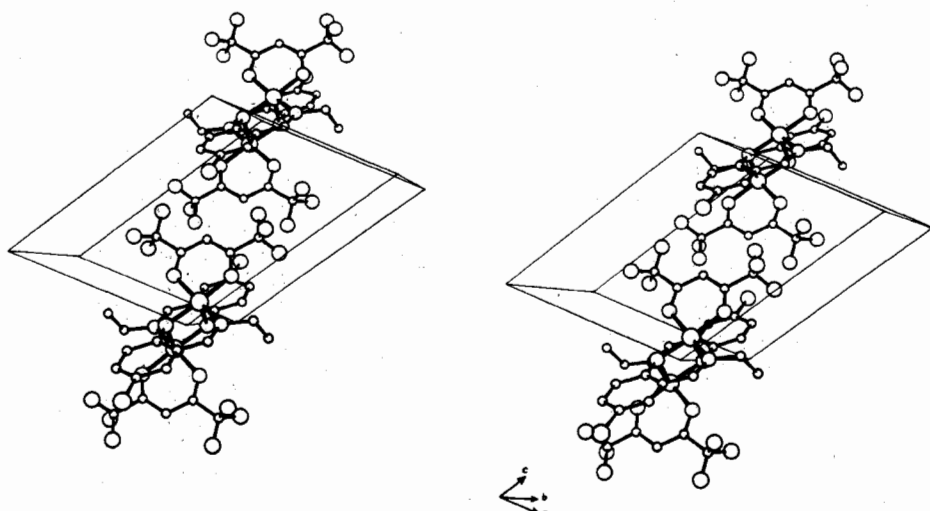
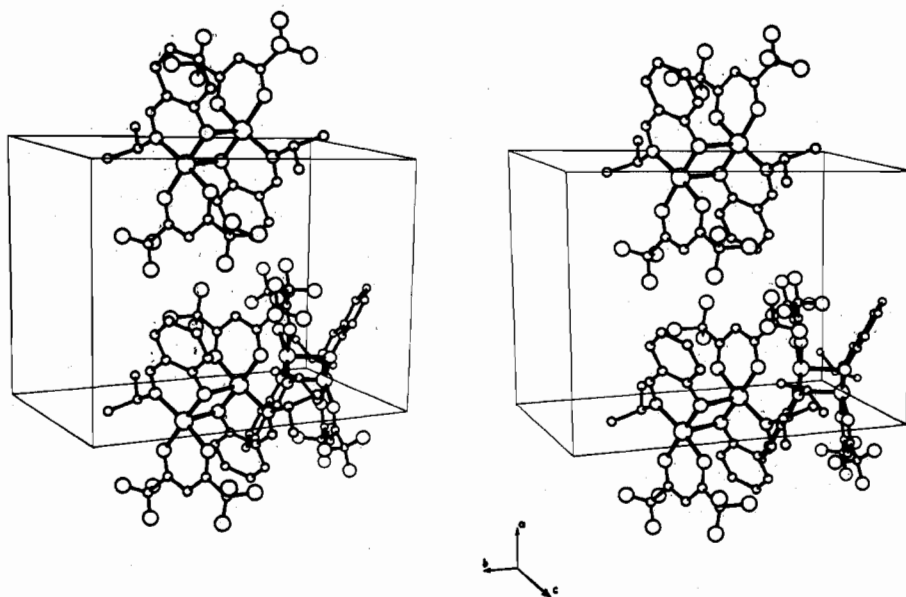
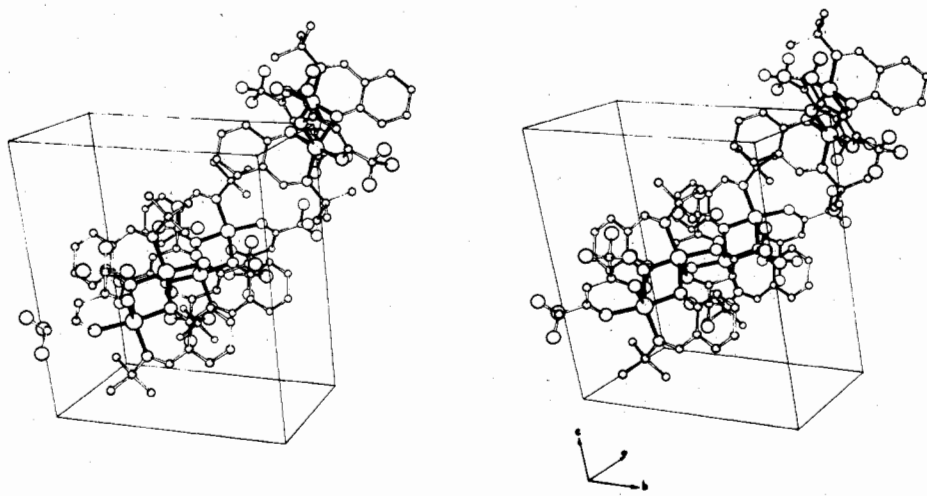
Figure 1. Stereopair view of 4a, $[\text{Cu}(\text{PrNaph})\text{NO}_3]_2$.Figure 2. Stereopair view of 4b, $[\text{Cu}(i\text{-PrSal})\text{thac}]_2$.Figure 3. Stereopair view of 4c, $[\text{Cu}(\text{PhSal})\text{hfa}]_2$.

Figure 4. Stereopair view of **4d**, $[\text{Cu}(\text{Et-5-ClSal})\text{hfa}]_2$.Figure 5. Stereopair view of **4e**, $[\text{Cu}(i\text{-PrSal})\text{hfa}]_2$.Figure 6. Stereopair view of **4f**, $[\text{Cu}(t\text{-BuSal})\text{hfa}]_2$.

pyramids joined at an edge of the base. The bridging oxygen atoms are joined to both copper atoms via short (1.91, 2.04 Å) bonds and the Cu–Cu separation is 3.027 (1) Å which

would be a relatively short distance for type 3 complexes.¹⁵ Complex **4b**, $[\text{Cu}(i\text{-PrSal})\text{thac}]_2$, contains discrete dimeric molecules, the nearest intermolecular contacts being between

Figure 7. Molecular packing in **4a**, $[\text{Cu}(\text{PrNaph})\text{NO}_3]_2$.Figure 8. Molecular packing in **4b**, $[\text{Cu}(i\text{-PrSal})\text{thac}]_2$.Figure 9. Molecular packing in **4c**, $[\text{Cu}(\text{PhSal})\text{hfa}]_2$.

Figure 10. Molecular packing in 4d, $[\text{Cu}(\text{Et}-5\text{-ClSal})\text{hfa}]_2$.Figure 11. Molecular packing in 4e, $[\text{Cu}(i\text{-PrSal})\text{hfa}]_2$.Figure 12. Molecular packing in 4f, $[\text{Cu}(t\text{-BuSal})\text{hfa}]_2$.

ligand fluorine atoms (3.28 \AA) and between a thac oxygen atom and phenyl carbons of an adjacent molecule (3.33 \AA). Here the β -diketone is chelated at the base of a distorted

square pyramid with two short ($1.95, 1.97 \text{ \AA}$) Cu–O bonds. The base of the square pyramid is distorted somewhat from planar to tetrahedral geometry (plane II, Table X), and the

Table VII. Bond Lengths (Å)

	4a	4b	4c	4d	4e	4f
Cu–O(1)	1.908 (1)	1.902 (1)	1.896 (1)	1.901 (1)	1.908 (1)	1.904 (3)
Cu–O(1')	2.040 (1)	2.437 (1)	2.391 (1)	2.368 (1)	2.298 (1)	2.098 (3)
Cu–O(2)	1.958 (1)	1.970 (1) ^a	1.945 (1)	1.953 (1)	1.958 (1)	1.943 (3)
Cu–O(3)	2.457 (1)	1.945 (1) ^a	1.990 (1)	2.000 (1)	2.008 (1)	2.131 (4)
Cu–N(1)	1.924 (1)	1.990 (1)	1.968 (1)	1.986 (1)	1.963 (1)	2.011 (3)
O(1)–C(2)	1.341 (2)	1.327 (1)	1.334 (2)	1.331 (1)	1.329 (2)	1.321 (5)
C(1)–C(2)	1.400 (3)	1.411 (2)	1.411 (3)	1.414 (2)	1.415 (2)	1.405 (6)
C(1)–C(6)	1.453 (3)	1.411 (1)	1.418 (3)	1.408 (2)	1.418 (3)	1.408 (6)
C(2)–C(3)	1.413 (3)	1.405 (2)	1.403 (3)	1.404 (2)	1.403 (2)	1.397 (6)
C(3)–C(4)	1.354 (3)	1.383 (1)	1.383 (3)	1.376 (2)	1.385 (3)	1.364 (7)
C(4)–C(5)	1.397 (3)	1.385 (0)	1.372 (4)	1.401 (2)	1.407 (3)	1.379 (8)
C(5)–C(6)	1.432 (3)	1.371 (0)	1.371 (3)	1.351 (2)	1.370 (3)	1.361 (7)
(a) $[\text{Cu}(\text{PrNaph})\text{NO}_3]_2$ (Continued)						
O(2)–N(2)		1.282 (2)		C(6)–C(10)		1.415 (3)
O(3)–N(2)		1.243 (2)		C(7)–C(8)		1.353 (3)
O(4)–N(2)		1.219 (2)		C(8)–C(9)		1.414 (3)
N(1)–C(11)		1.282 (2)		C(9)–C(10)		1.368 (3)
N(1)–C(12)		1.501 (2)		C(12)–C(13)		1.499 (3)
C(1)–C(11)		1.446 (3)		C(13)–C(14)		1.540 (3)
C(5)–C(7)		1.417 (3)				
(b) $[\text{Cu}(i\text{-PrSal})\text{thac}]_2$ (Continued)						
S–C(15)	1.718 (0)		C(8)–C(9)		1.535 (0)	
S–C(16)	1.695 (0)		C(8)–C(10)		1.535 (0)	
F(1)–C(11)	1.305 (1)		C(11)–C(12)		1.531 (0)	
F(2)–C(11)	1.313 (1)		C(12)–C(13)		1.366 (0)	
F(3)–C(11)	1.322 (1)		C(13)–C(14)		1.409 (0)	
O(2)–C(12)	1.268 (1)		C(14)–C(15)		1.459 (0)	
O(3)–C(14)	1.269 (1)		C(16)–C(17)		1.316 (0)	
N(1)–C(7)	1.287 (1)		C(17)–C(18)		1.415 (0)	
N(1)–C(8)	1.495 (1)		C(18)–C(15)		1.368 (0)	
C(1)–C(7)	1.430 (1)					
(c) $[\text{Cu}(\text{PhSal})\text{hfa}]_2$ (Continued)						
O(2)–C(15)	1.249 (2)		C(14)–C(15)		1.545 (3)	
O(3)–C(17)	1.256 (2)		C(15)–C(16)		1.387 (3)	
N(1)–C(7)	1.281 (2)		C(16)–C(17)		1.377 (3)	
N(1)–C(8)	1.453 (2)		C(17)–C(18)		1.536 (3)	
C(1)–C(7)	1.433 (3)		C(14)–F(1)		1.276 (3)	
C(8)–C(9)	1.367 (3)		C(14)–F(2)		1.301 (4)	
C(9)–C(10)	1.383 (3)		C(14)–F(3)		1.275 (3)	
C(10)–C(11)	1.354 (4)		C(18)–F(1')		1.253 (3)	
C(11)–C(12)	1.353 (4)		C(18)–F(2')		1.267 (3)	
C(12)–C(13)	1.393 (4)		C(18)–F(3')		1.248 (3)	
C(13)–C(8)	1.373 (3)					
(d) $[\text{Cu}(N\text{-Et}_5\text{ClSal})\text{hfa}]_2$ (Continued)						
Cl–C(5)	1.765 (1)		C(12)–C(13)		1.386 (2)	
O(2)–C(11)	1.260 (1)		C(13)–C(14)		1.536 (2)	
O(3)–C(13)	1.248 (1)		C(14)–F(1')		1.316 (2)	
N(1)–C(7)	1.280 (2)		C(14)–F(2')		1.282 (2)	
N(1)–C(8)	1.487 (2)		C(14)–F(3')		1.329 (2)	
C(1)–C(7)	1.428 (2)		C(10)–F(1)		1.328 (2)	
C(8)–C(9)	1.500 (2)		C(10)–F(2)		1.307 (2)	
C(10)–C(11)	1.532 (2)		C(10)–F(3)		1.324 (2)	
C(11)–C(12)	1.383 (2)					
(e) $[\text{Cu}(i\text{-PrSal})\text{hfa}]_2$ (Continued)						
O(2)–C(12)	1.264 (2)		C(13)–C(14)		1.396 (3)	
O(3)–C(14)	1.246 (2)		C(14)–C(15)		1.540 (3)	
N(1)–C(7)	1.274 (2)		C(11)–F(1)		1.227 (3)	
N(1)–C(8)	1.509 (2)		C(11)–F(2)		1.259 (4)	
C(1)–C(7)	1.444 (3)		C(11)–F(3)		1.257 (4)	
C(8)–C(9)	1.532 (3)		C(15)–F(1')		1.286 (3)	
C(8)–C(10)	1.547 (3)		C(15)–F(2')		1.266 (3)	
C(11)–C(12)	1.522 (3)		C(15)–F(3')		1.368 (4)	
C(12)–C(13)	1.368 (3)					
(f) $[\text{Cu}(t\text{-BuSal})\text{hfa}]_2$ (Continued)						
O(2)–C(13)	1.245 (6)		C(13)–C(14)		1.345 (7)	
O(3)–C(15)	1.225 (6)		C(14)–C(15)		1.408 (7)	
N(1)–C(7)	1.268 (6)		C(15)–C(16)		1.498 (7)	
N(1)–C(8)	1.503 (5)		C(12)–F(1)		1.253 (8)	
C(1)–C(7)	1.457 (6)		C(12)–F(2)		1.209 (7)	
C(8)–C(9)	1.540 (8)		C(12)–F(3)		1.271 (9)	
C(8)–C(10)	1.527 (8)		C(16)–F(1')		1.269 (7)	
C(8)–C(11)	1.530 (8)		C(16)–F(2')		1.286 (7)	
C(12)–C(13)	1.506 (7)		C(16)–F(3')		1.283 (7)	

^a O(2) and O(3) reversed for this compound.

Table VIII (Continued)

	(d) $[\text{Cu}(\text{N-Et-5-ClSal})\text{hfa}]_2$, (Continued)		
N(1)-C(7)-C(1)	128.2 (1)	C(12)-C(13)-C(14)	118.4 (1)
N(1)-C(8)-C(9)	111.4 (1)	C(13)-C(14)-F(1')	114.2 (1)
C(11)-C(10)-F(1)	109.5 (1)	C(13)-C(14)-F(2')	112.0 (1)
C(11)-C(10)-F(2)	112.9 (1)	C(13)-C(14)-F(3')	110.5 (1)
C(11)-C(10)-F(3)	113.5 (1)	F(1')-C(14)-F(2')	108.1 (1)
F(1)-C(10)-F(2)	108.0 (1)	F(1')-C(14)-F(3')	105.3 (1)
F(1)-C(10)-F(3)	105.0 (1)	F(2')-C(14)-F(3')	106.3 (1)
	(e) $[\text{Cu}(i\text{-PrSal})\text{hfa}]_2$, (Continued)		
Cu-O(2)-C(12)	128.3 (1)	F(2)-C(11)-F(3)	99.6 (3)
Cu-O(3)-C(14)	126.5 (1)	O(2)-C(12)-C(11)	114.5 (2)
Cu-N(1)-C(7)	122.6 (1)	O(2)-C(12)-C(13)	127.7 (2)
Cu-N(1)-C(8)	119.6 (1)	C(11)-C(12)-C(13)	117.8 (2)
C(7)-N(1)-C(8)	117.7 (2)	C(12)-C(13)-C(14)	120.6 (2)
N(1)-C(7)-C(1)	127.1 (2)	C(14)-C(15)-F(1')	115.7 (2)
N(1)-C(8)-C(9)	113.0 (2)	C(14)-C(15)-F(2')	113.0 (2)
N(1)-C(8)-C(10)	109.0 (2)	C(14)-C(15)-F(3')	108.5 (2)
C(9)-C(8)-C(10)	113.5 (2)	F(1')-C(15)-F(2')	111.9 (3)
C(12)-C(11)-F(1)	117.3 (2)	F(1')-C(15)-F(3')	103.6 (2)
C(12)-C(11)-F(2)	111.9 (3)	F(2')-C(15)-F(3')	102.9 (3)
C(12)-C(11)-F(3)	111.9 (3)	O(3)-C(14)-C(13)	128.3 (2)
F(1)-C(11)-F(2)	108.4 (3)	O(3)-C(14)-C(15)	114.5 (2)
F(1)-C(11)-F(3)	106.1 (3)	C(13)-C(14)-C(15)	117.1 (2)
	(f) $[\text{Cu}(t\text{-BuSal})\text{hfa}]_2$, (Continued)		
Cu-O(2)-C(13)	127.5 (4)	F(1)-C(12)-F(3)	101.4 (7)
Cu-O(3)-C(15)	125.2 (4)	F(2)-C(12)-F(3)	99.4 (7)
Cu-N(1)-C(7)	116.8 (4)	O(2)-C(13)-C(12)	113.3 (5)
Cu-N(1)-C(8)	124.6 (3)	O(2)-C(13)-C(14)	129.3 (5)
C(7)-N(1)-C(8)	118.7 (4)	C(12)-C(13)-C(14)	117.4 (6)
N(1)-C(7)-C(1)	128.2 (4)	C(13)-C(14)-C(15)	123.6 (5)
N(1)-C(8)-C(9)	107.7 (4)	O(3)-C(15)-C(14)	124.6 (5)
N(1)-C(8)-C(10)	112.3 (4)	O(3)-C(15)-C(16)	115.8 (5)
N(1)-C(8)-C(11)	107.3 (4)	C(14)-C(15)-C(16)	119.5 (6)
C(9)-C(8)-C(10)	110.0 (5)	C(15)-C(16)-F(1')	114.7 (6)
C(9)-C(8)-C(11)	110.1 (5)	C(15)-C(16)-F(2')	114.8 (5)
C(10)-C(8)-C(11)	109.5 (5)	C(15)-C(16)-F(3')	112.4 (5)
C(13)-C(12)-F(1)	117.9 (6)	F(1')-C(16)-F(2')	105.9 (6)
C(13)-C(12)-F(2)	115.4 (6)	F(1')-C(16)-F(3')	104.0 (5)
C(13)-C(12)-F(3)	112.5 (8)	F(2')-C(16)-F(3')	103.9 (6)
F(1)-C(12)-F(2)	107.7 (8)		

^a O(2) and O(3) reversed for this compound.

square pyramids joined as in complexes **4b**, **4d**, and **4e**.

Complex **4d**, $[\text{Cu}(\text{Et-5-ClSal})\text{hfa}]_2$, consists of discrete dimeric molecules with close copper to chlorine (3.15 Å) and fluorine to fluorine (3.08–3.14 Å) contacts. The β -diketone is chelated at the base of a distorted square pyramid with short (1.95, 2.00 Å) but significantly different Cu–O bonds. Though significantly distorted toward trigonal-bipyramidal geometry, the metal geometry is decidedly closer to square pyramidal, and the copper atom is raised 0.13 Å above the pyramid base. The bridging Cu–O bonds (2.37 Å) and the Cu–Cu separation (3.143 (1) Å) are shorter than in complexes **4b** and **4c** but longer than in the others. The distorted square-pyramidal monomeric halves of the molecule are linked in the same fashion as in complexes **4b**, **4c**, and **4e**.

Complex **4e**, $[\text{Cu}(i\text{-PrSal})\text{hfa}]_2$, consists of discrete dimeric molecules with fluorine contacts being the closest (3.02–3.08 Å) intermolecular approaches. The β -diketone is chelated at the base of a square pyramid with two short (1.96, 2.01 Å) but significantly different Cu–O bonds. The square-pyramidal metal geometry is slightly distorted toward trigonal-bipyramidal geometry, less so than for **4d** and (especially) **4b** but more than for **4c**. The bridging Cu–O bonds (2.30 Å) and the Cu–Cu separation (3.119 (1) Å) are shorter than in complexes **4b**, **4c**, and **4d** but longer than in **4a** and **4f**. The distorted square pyramids are linked to form a dimer as in complexes **4b**, **4c**, and **4d**.

Complex **4f**, $[\text{Cu}(t\text{-BuSal})\text{hfa}]_2$, contains discrete dimeric molecules with fluorine to (*tert*-butyl) carbon contacts being the closest intermolecular approaches. The β -diketone is chelated with one short (1.94 Å) and one markedly longer

(2.13 Å) Cu–O bond. The short bond is at one apex and the long bond at one equatorial point of a distorted trigonal bipyramidal. Although the metal geometry is slightly distorted (essentially) toward square pyramidal, this is the only one of the complexes with essentially a trigonal-bipyramidal configuration. The bridging oxygen atoms are joined to the two copper atoms with relatively short (1.90, 2.10 Å) but markedly different bonds. The bridging Cu–O bonds (2.10 Å) and the Cu–Cu separation (3.089 (1) Å) are the shortest observed for these complexes, except **4a** $[\text{Cu}(\text{PrNaph})\text{NO}_3]_2$. The dimeric molecule is formed from the monomeric trigonal-bipyramidal fragments by joining the apex of each one to one equatorial point of the other. Extrapolation of the change in the gross geometry of **4b**, **4c**, and **4d** to that of **4f** would produce a structure very close to that of **4a**.

Weak magnetic interactions have been observed to occur in dimeric molecules separated from one another except for weak intermolecular hydrogen bonds, but the weak interdimer contacts observed here are not likely to lead to significant magnetic effects, compared with larger intradimer interactions, nor to marked structural perturbations. The molecules may therefore be considered to be magnetically isolated, except in the cases where the intradimer links are weakest (discussed below). The Cu–Cl contact in **4d**, $[\text{Cu}(\text{Et-5-ClSal})\text{hfa}]_2$, is just at the van der Waals contact distance²⁸ and is likely to cause a small perturbation of the intramolecular magnetic exchange and perhaps of the molecular structure as well.

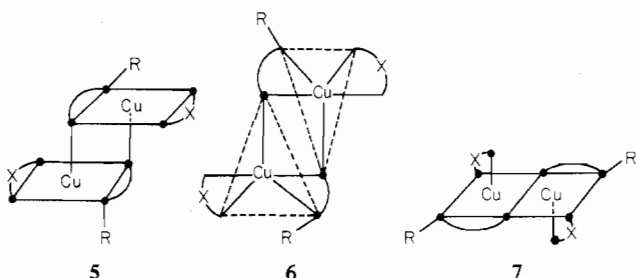
Intramolecular steric interactions, electronic factors,²⁹ and packing in the crystalline lattice can influence the changes in structures observed in the series of binuclear complexes, but

Table IX. Closest Intermolecular Distances

Molecule 1	Molecule 2	Dist, Å	Symm transformn	Molecule 1	Molecule 2	Dist, Å	Symm transformn
4a, [Cu(PrNaph)NO₃]₂							
O(3)	C(10)	3.435	x - 1, y - 1, z	N(2)	C(8)	3.429	1 - x, -y, -z
	C(8)	3.467	1 - x, -y, -z		C(5)	3.415	1 - x, 1 - y, -z
	C(9)	3.480	1 - x, -y, -z		C(7)	3.400	1 - x, -y, -z
O(4)	C(14)	3.441	x - 1, y - 1, z		C(6)	3.564	1 - x, 1 - y, -z
N(1)	C(8)	3.532	1 - x, -y, -z				
4b, [Cu(i-PrSal)thac]₂							
F(2)	C(4)	3.544	x, y, 1 + z	O(3)	C(6)	3.331	1 - x, -y, -z
F(3)	F(3)	3.282	1 - x, 1 - y, 1 - z		C(14)	3.502	1 - x, -y, -z
	C(16)	3.465	x, 1 + y, z		C(9)	3.440	-x, -1 - y, -z
	C(17)	3.569	x, 1 + y, z		C(10)	3.568	1 - x, -1 - y, -z
4c, [Cu(PhSal)hfa]₂							
F(1)	F(2')	2.972	x - 1, y, z	F(3')	F(3')	3.109	1 - x, 1 - y, 1 - z
F(2)	O(2)	3.301	1 - x, -y, 1 - z		C(4)	3.524	-x, -y, -1 - z
F(3)	C(4)	3.311	x, 1 + y, 1 + z		C(5)	3.541	-x, -y, -1 - z
	F(3')	3.403	1 - x, 1 - y, 1 - z				
4d, [Cu(N-Et-5-ClSal)hfa]₂							
Cu	C1	3.147	-x, y, -z	F(2)	F(1')	3.298	1 - x, 1 - y, 1 - z
Cl	O(2)	3.362	-x, -1 - y, -z		F(1')	3.089	1 - x, 1 - y, 1 - z
	O(3)	3.479	-x, -1 - y, -z		F(3')	3.185	1 - x, 1 - y, 1 - z
F(1)	F(1)	3.241	-x, -y, -z		C(6)	3.386	x + 1, y + 1, z + 1
	F(2)	3.269	-x, -y, -z		C(5)	3.457	x + 1, y + 1, z + 1
F(2)	F(2')	3.143	x - 1, y, z	F(2')	C(9)	3.308	x + 1, y, z
4e, [Cu(i-PrSal)hfa]₂							
Cu	C(10)	3.299	x, 1/2 - y, z - 1/2	F(1')	C(4)	3.411	1 + x, y, z
F(1)	F(3')	3.356	1 - x, -y, -z		F(3)	3.020	x, y, z - 1
	C(6)	3.356	1 + x, y, z		C(8)	3.351	x, y, z - 1
	C(5)	3.504	1 + x, y, z		C(9)	3.551	x, y, z - 1
F(1')	F(3)	3.079	x, y, z - 1	O(3)	C(10)	3.488	x, 1/2 - y, z - 1/2
4f, [Cu(t-BuSal)hfa]₂							
F(1)	F(1)	3.532	1 - x, -1 - y, -z	F(1')	C(9)	3.567	1 - x, -y, -z
F(2)	F(1')	3.503	1 - x, -y, -z		F(2')	3.142	1 - x, -y, -z
F(3)	C(5)	3.348	x, y - 1, z		C(1)	3.252	1 - x, -y, -z
F(1')	C(13)	3.379	1 - x, -y, -z		N(1)	3.389	1 - x, -y, -z
	O(2)	3.395	1 - x, -y, -z				

these effects can only be partially separated. The molecular geometry varies gradually from one dimer to another. The bridging bond, Cu-O(1'), decreases in length in the order **4b** (thac) > **4c** (hfa) > **4d** (hfa) > **4e** (hfa) > **4f** (hfa) > **4a**, while the Cu-O(3) length decreases in the same order. This is also the sequence of increasing ligand electronegativity, thac < hfa < NO₃, and suggests that strong binucleation is enhanced by ligand electronegativity. The dimeric form of the N-methylsalicylaldimine complex (X = N-methylsalicylaldimine, R = CH₃, R' = H) fits into this series, having weak Cu-O(1') bonds.³⁰ The difference in ligand "bite" of NO₃, on one hand, and that of hfa and thac, on the other, is another factor of unknown importance. Within the hfa series, steric effects should be the most important factor in determining structural features (vide infra) but packing effects cannot be ignored.

The observed trend of the geometry about the individual metal atoms is from **5** approximately square pyramidal and



dimerized at the apices and one corner (**4b**, [Cu(i-PrSal)thac]₂; **4c**, [Cu(PhSal)hfa]₂; **4d**, [Cu(Et-5-ClSal)hfa]₂; **4e**, [Cu(i-PrSal)hfa]₂) through **6** of approximately trigonal-bipyramidal character, again dimerized through an apex and a base corner

(**4f**, [Cu(t-BuSal)hfa]₂), and back to approximately square-pyramidal **7**, but dimerized via the bases of the pyramids (**4a**, [Cu(PrNaph)NO₃]₂). In each case, the base pyramids are coplanar (**4a**) or parallel (**4b**-**4f**). This trend also may be rooted in ligand electronegativity, though again steric, and perhaps packing, effects play a part. These geometry changes are quantified by the planarity, or lack of same, of four analogous sets of atoms for each complex (Table X) and the interplanar angles. These data show the same trend and clearly require different orbital configurations. Because of the relatively large sample of compounds chosen, it is evident that the variation is gradual over the series, rather than abrupt.

Within a more restricted group of complexes (X = hfa), the observed trend also parallels the size of the alkyl substituent approximately: **4c** (phenyl) > **4d** (ethyl) > **4e** (isopropyl) > **4f** (tert-butyl). Distortion toward trigonal-bipyramidal geometry would accommodate increasingly large substituents on both ligands without requiring longer bridging (Cu-O(1')) bonds. However, the steric trend may be fortuitous, in the absence of more data, because of the unknown effect of the close Cl-Cu approach in **4d** [Cu(Et-5-ClSal)hfa]₂ and evidence of possible phase changes in **4f** [Cu(t-BuSal)hfa]₂.¹⁸ Physical measurements on **4f** [Cu(t-BuSal)hfa]₂ have been interpreted in terms of a phase change which changes the molecular structure to type **6**, below 100 K. If correct, this implies that packing effects are probably as important as, or more so than, the intramolecular crowding due to the bulky tert-butyl group.

Each copper atom is chelated to a β-diketone ligand in the thac and hfa dimers and the metal atom is five-coordinated with one long metal-ligand bond. This observation fits in with the structures of a number of other copper(II) complexes which

Table X. Coefficients of Least-Squares Planes $AX + BY + CZ = D$ for 4a-4f

Plane	Atoms		A	B	C	D	Distances, Å
I	Cu, Cu', O(1), O(1')	4a	-0.032	-0.998	-0.046	0	
		4b	0.293	-0.376	-0.879	0	
		4c	-0.652	-0.080	-0.754	0	
		4d	-0.731	-0.579	-0.361	0	
		4e	0.643	-0.254	-0.722	0	
		4f	0.725	0.125	-0.677	0	
II	O(1), O(1'), O(2), N(1)	4a	-0.298	0.953	-0.062	0.006	O(1), -0.44; O(1'), 0.43; O(2), -0.39; N(1), 0.40; Cu, -0.11
		4b	-0.904	-0.283	-0.321	-1.426	O(1), 0.28; O(2), -0.29; O(3), 0.27; N(1), -0.26; Cu, -0.16
		4c	0.546	0.687	-0.480	1.283	O(1), -0.07; O(2), -0.06; O(3), 0.07; N(1), 0.06; Cu, -0.12
		4d	-0.532	0.705	-0.469	-1.300	O(1), 0.13; O(2), 0.13; O(3), -0.14; N(1), -0.13; Cu, 0.13
		4e	-0.009	0.918	-0.397	1.247	O(1), -0.08; O(2), -0.07; O(3), 0.08; N(1), 0.07; Cu, -0.14
		4f					
III	C(1)-C(7), Cu, O(1), N(1)	4a	0.439	-0.848	-0.298	0.586	C(1), -0.05; C(2), -0.07; C(3), 0.07; C(4), 0.13; C(5), 0.13; C(6), -0.04; Cu, 0.10; O(1), -0.19; N(1), 0.07; C(7), -0.05
		4b	-0.718	-0.225	-0.659	-1.045	C(1), 0.03; C(2), 0.08; C(3), 0; C(4), -0.06; C(5), -0.07; C(6), -0.03; Cu, -0.25; O(1), 0.19; N(1), 0.02; C(7), 0.08
		4c	0.541	0.824	-0.166	1.098	C(1), 0; C(2), -0.04; C(3), -0.02; C(4), 0.03; C(5), 0.05; C(6), 0.04; Cu, 0.22; O(1), -0.16; N(1), -0.06; C(7), -0.07
		4d	-0.569	0.437	-0.697	-1.024	C(1), 0.03; C(2), 0.07; C(3), 0.02; C(4), -0.05; C(5), -0.07; C(6), -0.04; Cu, -0.24; O(1), 0.17; N(1), 0.05; C(7), 0.07
		4e	0.401	0.817	-0.413	1.004	C(1), -0.01; C(2), 0.06; C(3), -0.05; C(4), 0.04; C(5), 0.09; C(6), 0.06; Cu, 0.29; O(1), -0.18; N(1), -0.08; C(7), -0.11
		4f	0.971	-0.138	-0.193	0.289	C(1), -0.06; C(2), -0.17; C(3), -0.11; C(4), 0.09; C(5), 0.20; C(6), 0.11; Cu, 0.59; O(1), -0.33; N(1), -0.11; C(7), -0.20
IV	Cu, O(2), O(3), O(4), N(2)	4a	0.988	-0.102	-0.115	0.837	Cu, 0.05; O(2), -0.06; O(3), -0.03; N(2), -0.02; O(4), -0.06
		4b	-0.969	-0.106	-0.224	-1.447	Cu, 0.05; O(2), -0.04; O(3), -0.06; C(12), -0.01; C(13), 0.04; C(14), 0.01
		4c	0.502	0.700	-0.508	1.236	Cu, -0.05; O(2), 0.05; O(3), 0.04; C(15), 0; C(16), -0.04; C(17), 0.01
		4d	-0.438	0.811	-0.388	-1.109	Cu, -0.04; O(2), 0.05; O(3), 0.01; C(10), -0.03; C(11), 0.02; C(12), -0.01
		4e	-0.969	-0.106	-0.224	-1.447	Cu, 0.05; O(2), -0.04; O(3), -0.06; C(12), -0.01; C(13), 0.04; C(17), 0.01
		4f	-0.694	-0.400	-0.599	-1.287	Cu, 0.11; O(2), -0.08; O(3), -0.12; C(13), -0.02; C(14), 0.07; C(15), 0.04

Interplanar Angles, Deg

	I,II	I,III	I,IV	II,III	II,IV	III,IV
4a		32.2	85.7			56.3
4b	82.9	63.1	87.3	22.5	12.2	29.9
4c	87.2	72.9	90.0	19.7	3.1	21.1
4d	81.4	65.5	89.5	20.4	9.3	29.1
4e	87.3	69.6	86.7	24.4	6.1	29.7
4f		35.1	81.5			59.8

contain two or three hfa ligands per copper atom and which are six-coordinated but distorted from octahedral symmetry mainly by axial bond elongation: four short (2.01 Å) and two long bonds (2.16, 2.20 Å) for three hfa ligands in $[\text{Cu}(\text{hfa})_3]^{2-}$,⁸ four short (1.97 Å for Cu-O and 2.00 Å for Cu-N) and two long bonds (2.30 Å for Cu-O) for two hfa ligands in $[\text{Cu}(\text{hfa})_2\text{bpy}]$,⁹ and four short (1.99, 2.06 Å for Cu-N) and two very long bonds (2.79 Å for Cu-O) in $[\text{Cu}(\text{hfa})_2$

$(\text{NH}_2(\text{CH}_2)_2\text{N}(\text{CH}_3)_2)_2]$ ¹¹ where hfa is not chelated. Four-coordinated structures are the most common with bidentate Schiff bases and halogen ligands (3) in place of hfa, thac, or NO_3^- , as in $[\text{Cu}(\text{EtSal})\text{Cl}]_2$,^{14,15} with all four bonds short.

The well-known tendency of $\text{Cu}(\text{hfa})_2$ to become six-coordinated by combining with two monodentate or one bidentate Lewis base^{3-11,29} appears to be reduced to a preference for

five-coordination when there is only one hfa ligand per copper atom. This preference for five-coordination with one elongated bond is emulated by a wider range of mono-, bi-, and tetranuclear complexes containing one hfa, thac, or 1,1,1-trifluoro-2,4-pentanedione ligand.¹² Complexes of type **2** (CuTSB) M(hfa)_2 related to **4a–8** represent the extreme case of zero hfa ligands on one copper atom which then prefers four-coordination.

The dimeric type **3** complexes $[\text{Cu}(\text{RSal})\text{X}_2]_2$ ($\text{X} = \text{Cl}, \text{Br}$) generally exhibit fairly strong antiferromagnetic interactions, as do the $[\text{Cu}(\text{RSal})\text{NO}_3]_2$ complexes (types **4**, **7**). $[\text{Cu}(t\text{-BuSal})\text{hfa}]_2$ (**4f**) also exhibits relatively strong antiferromagnetic interactions, at least down to about 100 K, where a presumed structural change occurs. However, $[\text{Cu}(i\text{-PrSal})\text{hfa}]_2$ (**4e**) and a series of related hfa dimers have room-temperature magnetic moments near but slightly below (1.71–1.80 μ_b) the normal values expected for simple paramagnets, and the ESR spectra indicate the presence of $S = 1$ state species.¹⁸ Thus weak antiferromagnetic, or possibly ferromagnetic, interactions exist in these complexes. Although the magnetic properties of $[\text{Cu}(i\text{-PrSal})\text{thac}]_2$, $[\text{Cu}(\text{PhSal})\text{hfa}]_2$, and $[\text{Cu}(\text{Et-5-ClSal})\text{hfa}]_2$ (**4b–4d**) are presently unknown, it seems safe to predict normal room-temperature moments with weak antiferromagnetic or ferromagnetic interactions. The strength and sign of the interaction (J , negative for antiferromagnetism, positive for ferromagnetism) should be determined by a combination of factors, the most important of which are the Cu–O–Cu bridging angle,³¹ a decrease in which favors a less negative J value, the Cu–O bridging bond, weakening of which will minimize all exchange pathways, and the distortion from planarity of the four strongly bonded ligand atoms. A more extensive structural and magnetic study will serve to elucidate magnetic exchange mechanisms in such complexes.

Further work along these lines should explain the causes of binucleation in mixed-ligand and unmixed-ligand complexes in general, many of which are binuclear but need not be, or could be binuclear but are not.^{12,32–36}

Acknowledgment. Support received for instrumentation under NSF Grant GP-41679 is gratefully acknowledged.

Registry No. **4a**, 60104-19-0; **4b**, 60104-20-3; **4c**, 60104-21-4; **4d**, 60104-22-5; **4e**, 56371-77-8; **4f**, 56390-73-9.

Supplementary Material Available: Listings of structure factor

amplitudes (64 pages). Ordering information is given on any current masthead page.

References and Notes

- (1) S. J. Gruber, C. M. Harris, and E. Sinn, *J. Chem. Phys.*, **49**, 2183 (1968); *J. Inorg. Nucl. Chem.*, **30**, 1805 (1969); *Inorg. Chem.*, **7**, 268 (1968).
- (2) C. M. Harris, H. R. H. Patil, and E. Sinn, *Inorg. Chem.*, **6**, 1102 (1967).
- (3) G. T. Morgan and J. D. M. Smith, *J. Chem. Soc.*, 912 (1926).
- (4) W. R. Walker, *Aust. J. Chem.*, **14**, 161 (1961).
- (5) L. L. Funck and T. R. Ortolano, *Inorg. Chem.*, **7**, 567 (1968).
- (6) A. F. Garito and B. B. Wayland, *J. Am. Chem. Soc.*, **91**, 866 (1969).
- (7) W. Partenheimer and R. S. Drago, *Inorg. Chem.*, **9**, 47 (1970).
- (8) M. R. Truter and B. L. Vickery, *J. Chem. Soc., Dalton Trans.*, 395 (1972).
- (9) M. V. Veidis, G. H. Schreiber, T. E. Gough, and G. J. Palenik, *J. Am. Chem. Soc.*, **91**, 1859 (1969).
- (10) D. E. Fenton, R. S. Nyholm, and M. R. Truter, *J. Chem. Soc., Dalton Trans.*, 1577 (1975).
- (11) M. A. Bush and D. E. Fenton, *J. Chem. Soc. A*, 2446 (1971).
- (12) D. P. Freyberg and E. Sinn, to be submitted for publication.
- (13) N. B. O'Bryan, T. O. Maier, I. C. Paul, and R. S. Drago, *J. Am. Chem. Soc.*, **95**, 6640 (1973).
- (14) E. Sinn and C. M. Harris, *Coord. Chem. Rev.*, **4**, 391 (1969), and references therein.
- (15) E. Sinn and W. T. Robinson, *J. Chem. Soc., Chem. Commun.*, 359 (1972); R. M. Countryman, W. T. Robinson, and E. Sinn, *Inorg. Chem.*, **13**, 2013 (1974).
- (16) R. J. Butcher and E. Sinn, *J. Chem. Soc., Chem. Commun.*, 832 (1975).
- (17) E. Sinn, *Inorg. Chem.*, **15**, 366 (1976).
- (18) H. Yokoi and M. Chikira, *J. Am. Chem. Soc.*, **97**, 3975 (1975).
- (19) J. O. Miners, E. Sinn, R. B. Coles, and C. M. Harris, *J. Chem. Soc., Dalton Trans.*, 1149 (1972).
- (20) W. R. Walker and N. C. Li, *J. Inorg. Nucl. Chem.*, **27**, 2255 (1965).
- (21) P. W. R. Corfield, R. J. Doedens, and J. A. Ibers, *Inorg. Chem.*, **6**, 197 (1967).
- (22) D. T. Cromer and J. T. Waber, "International Tables for X-Ray Crystallography", Vol. IV, Kynoch Press, Birmingham, England, 1974.
- (23) R. F. Stewart, E. R. Davidson, and W. T. Simpson, *J. Chem. Phys.*, **42**, 3175 (1965).
- (24) D. T. Cromer and J. A. Ibers, "International Tables for X-Ray Crystallography", Vol. IV, Kynoch Press, Birmingham, England, 1974.
- (25) D. P. Freyberg, G. M. Mockler, and E. Sinn, *J. Chem. Soc., Dalton Trans.*, 447 (1976).
- (26) M. Elder, *Inorg. Chem.*, **8**, 2103 (1969).
- (27) Supplementary material.
- (28) A. Bondi, *J. Chem. Phys.*, **68**, 441 (1964).
- (29) D. R. McMillin, R. S. Drago, and J. A. Nusz, *J. Am. Chem. Soc.*, **98**, 3120 (1976).
- (30) D. Hall, S. V. Sheat, and T. N. Waters, *J. Chem. Soc.*, 460 (1968).
- (31) D. J. Hodgson, *Prog. Inorg. Chem.*, **19**, 173 (1975).
- (32) D. Hall and T. N. Waters, *J. Chem. Soc.*, 2644 (1960).
- (33) E. N. Baker, D. Hall, A. J. McKinnon, and T. N. Waters, *Chem. Commun.*, 134 (1967).
- (34) R. W. Klubber, *Inorg. Chem.*, **4**, 107 (1965); T. S. Moore and M. W. Young, *J. Chem. Soc.*, 2694 (1932).
- (35) M. F. Farona, D. C. Perry, and H. A. Kuska, *Inorg. Chem.*, **7**, 2415 (1968).
- (36) U. Doraswamy and P. K. Bhattacharya, *J. Inorg. Nucl. Chem.*, **37**, 1665 (1975).